

## Crystallization of Eutectic Microstructures from Oxide and Carbide Melts

V. S. Stubican

Department of Material Sciences, The Pennsylvania State University, University Park, PA 16802, USA

The theoretical aspect of the directional solidification is briefly described. Two different experimental techniques were used for the production of directionally solidified high refractory oxide and carbide eutectics. Microstructure, crystallography, mechanical properties and mechanism of failure were investigated. Some of the investigated eutectics retain considerable strength at elevated temperature, whereas the majority of alloys and sintered oxide bodies show rapid loss in strength. Eutectic in the system  $B_4C-SiC$  shows exceptionally high wear resistance.

### SOLIDIFICATION OF EUTECTIC MELTS

When a melt of exactly the eutectic composition is solidified, two solid phases (in a binary system) form at the liquidus temperature and all of the liquid disappears before the temperature decreases further. It was already known since the 1920's<sup>1</sup> that by controlling solidification (removing heat preferentially from one direction) a microstructure can be produced which consists of a matrix phase within which is dispersed an aligned second phase. The second phase may be in the form of needles, rods or two phases can occur as alternate lamellae. The phases can be thought of as one single crystal imbedded in a matrix of another single crystal.

It is now well established that the two phases grow simultaneously<sup>2</sup> so that their common interfaces would be perpendicular to the solid-liquid interface. Each lamella has its own solid-liquid interface. It follows that the liquid in front of each lamella becomes enriched in the major component of the neighboring lamellae as shown in Figure 1 and that transverse diffusion of both components must take place. It has been observed and to a certain degree explained theoretically<sup>3</sup>, that the planar front growth is necessary to obtain normal eutectic microstructures. The condition for the breakdown of the planar interface is given by<sup>4</sup>

$$G < \frac{\Delta T_f \cdot R}{D} \quad (1)$$

where  $G$  is the temperature gradient,  $D$  is diffusion coefficient in the liquid,  $R$  is the growth rate and  $\Delta T_f$  is the freezing range of the mixture. To obtain the planar front growth and to produce well-aligned eutectic microstructures, it is then necessary to use steep temperature gradients, slow growth rates and very pure starting materials. Non-planar liquid-solid interface results in a

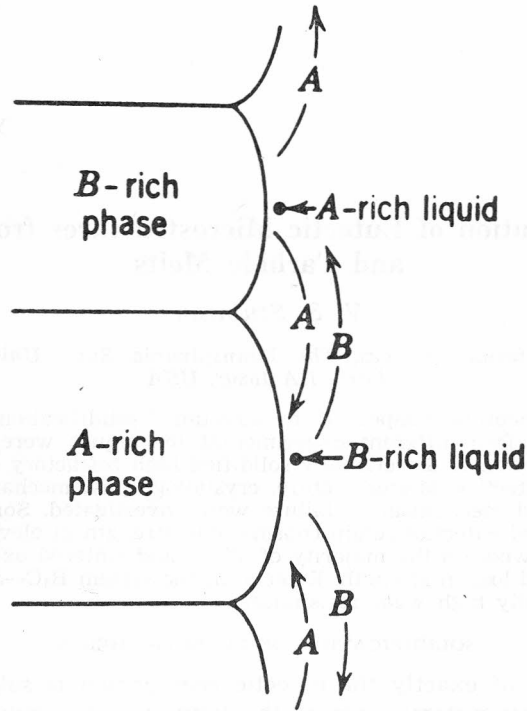


Figure 1. Diffusion paths for the growth of a lamellar eutectic. Ref. 3.

colony microstructure in which the interface breaks down into regions of high curvature separated by higher concentration of impurities.

It has been shown experimentally and has been explained theoretically<sup>5</sup> that in the eutectic microstructures the distance between the lamellae or rods ( $\lambda$ ) depends on the rate of solidification ( $R$ ) and that the relationship is

$$\lambda \propto R^{-1/2} \quad (2)$$

Most eutectic systems show a strong preference for a rod form or lamellae form of microstructure. This behavior is dependent on differences in the total solid-solid interfacial energy, which in turn is partly dependent on the relative volumes of the two eutectic phases. It is easy to derive on geometrical grounds<sup>6</sup> that if the relative volume fraction ( $V_F$ ) of two phases is less than 0.28 minor phase will grow in the form of rods. Lamellar type of microstructures can be expected if  $V_F > 0.28$ . On Figure 2 rod to lamellar morphology change in terms of interfacial area/unit volume change for several metallic eutectics is shown.

Preferred crystallographic orientations are often formed during controlled solidification of eutectic melts. It seems that in most cases the preferred orientations which develop are associated with low values of the interfacial energies and with the similarity of atomic densities of the interfacial planes<sup>7</sup>. It has been postulated<sup>8</sup> that to obtain nonfaceted growth\*, a factor  $\alpha$  should be less than 2. Factor  $\alpha$  was defined as:

\* Normal eutectic microstructures contain nonfaceted phases.

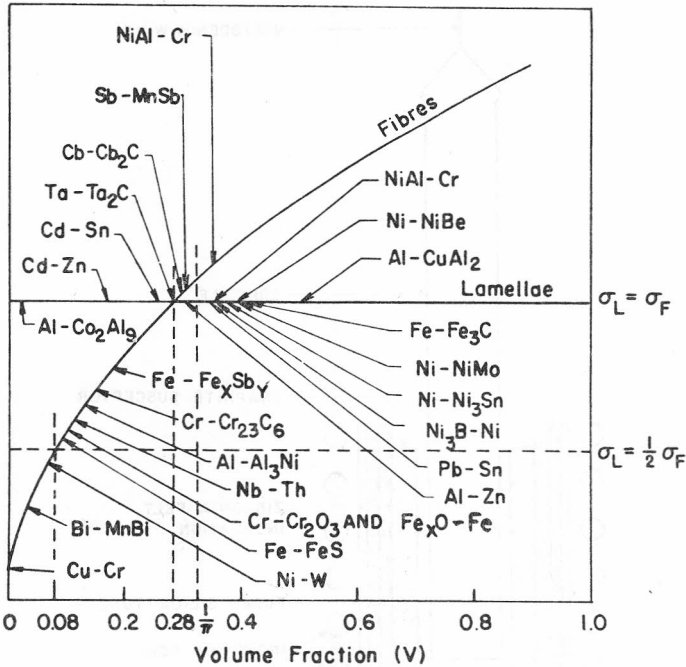


Figure 2. Rod to lamellar morphology change in terms of interfacial area/unit volume. Ref. 6.

$$\alpha = Q (\Delta S_F / R) \quad (3)$$

where  $Q$  is a crystallographic factor always less than or equal to one,  $\Delta S_F$  is the entropy of melting and  $R$  is the gas constant. Most metals and organic materials have low entropies of melting so that the condition  $\alpha < 2$  is easily met. Refractory oxides and carbides have high entropies of fusion and should show faceted growth. However, this is not the case and normal eutectic microstructures can be obtained in most refractory oxide systems.

#### EXPERIMENTAL METHODS

Two experimental methods were used to solidify oxide-oxide and carbide-carbide eutectics. There are (i), a modified Bridgman-Starkbarger method<sup>9,10</sup>, and (ii), a floating molten zone technique<sup>11</sup>. The first technique requires a furnace similar to that shown on Figure 3. Ingots are directionally solidified by lowering the loaded crucible, suspended from the upper traveling head of the furnace, by an Mo wire through the susceptor at the desired solidification rate. Because of the difficulty of measuring the actual growth rate of the ingot, it is assumed that the rate of growth is equal to the lowering rate of the crucible, i.e. the solidification rate. The lowering rate of the crucible is usually 0.5–30 cm/hr and the furnace is capable of reaching temperatures up to  $\sim 2500^\circ\text{C}$ . In our experiments the melting temperatures were  $\approx 50^\circ\text{C}$  above the eutectic liquidus. The thermal gradient at the eutectic liquidus temperature, determined by a W-Re thermocouple, was  $\approx 200^\circ\text{C}/\text{cm}$ . All melting and solidification procedures were conducted in argon. With the floating zone technique temperature gradients of 500–1500  $^\circ\text{C}/\text{cm}$  can be obtained. The actual heating of the presintered rod is accomplished by radiation from a small carbon ring susceptor and the molten zone is only 3–4 mm thick.

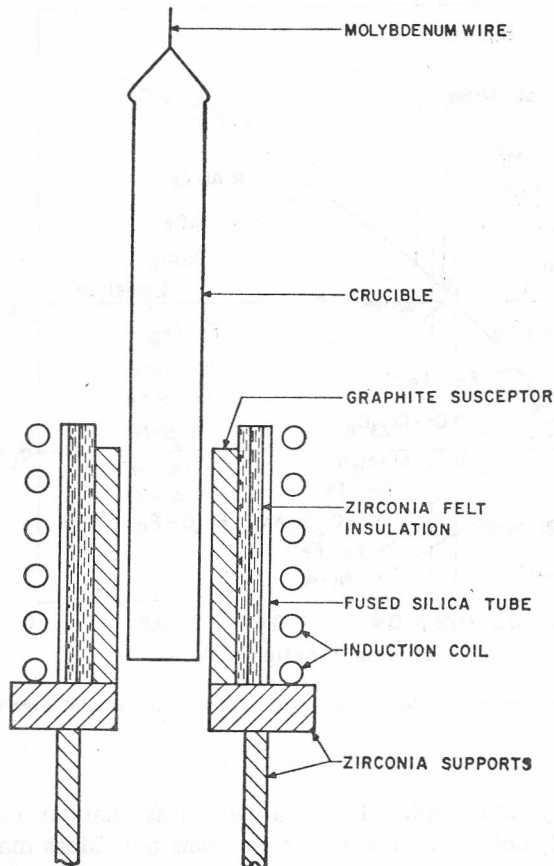


Figure 3. Interior layout of solidification furnace. Ref. 13.

The resulting ingots can be sectioned and used for optical and x-ray investigations. With both techniques it is possible to obtain large ingots which can be used for the investigations of mechanical, electrical, optical, magnetic or thermal properties.

#### REFRACTORY OXIDE AND CARBIDE EUTECTICS

##### *Microstructure*

The following refractory oxide eutectics were directionally solidified:  $\text{Al}_6\text{Si}_2\text{O}_{13}$  (mullite)- $\text{Al}_2\text{O}_3$ <sup>10</sup>,  $\text{MgAl}_2\text{O}_4$ - $\text{Al}_2\text{O}_3$ <sup>12</sup>,  $\text{MgO}$ - $\text{MgAl}_2\text{O}_4$ <sup>13</sup>,  $\text{ZrO}_2$ - $\text{MgO}$ <sup>14</sup>,  $\text{TiO}_2$ - $\text{MgO}$ <sup>15</sup>,  $\text{ZrO}_2$ - $\text{CaZrO}_3$ <sup>10,15</sup>,  $\text{ZrO}_2$ - $\text{SrZrO}_3$ <sup>15</sup>,  $\text{CaO}$ - $\text{MgO}$ <sup>10,15</sup>,  $\text{Al}_2\text{O}_3$ - $\text{ZrO}_2$ <sup>16</sup>,  $\text{Al}_2\text{O}_3$ - $\text{Y}_2\text{O}_3$ <sup>9</sup>. Only one carbide system  $\text{SiC}$ - $\text{B}_4\text{C}$  was directionally solidified. Normal eutectic microstructures, lamellar, rod or fibrous type could be produced with most high melting oxide eutectics by using directional solidification. For example, the eutectic between  $\text{MgO}$  and  $\text{MgAl}_2\text{O}_4$  is an attractive candidate for directional solidification; the phase diagram is shown in Figure 4. The eutectic is at 45 wt %  $\text{MgO}$  and 55 wt %  $\text{M}_2\text{O}_3$  and has a liquidus temperature of 1995°C. This composition yields  $\approx 14$  vol. %  $\text{MgO}$ , so that on

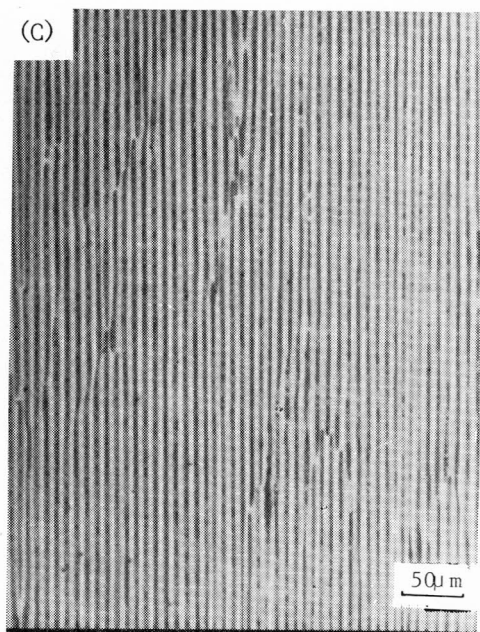
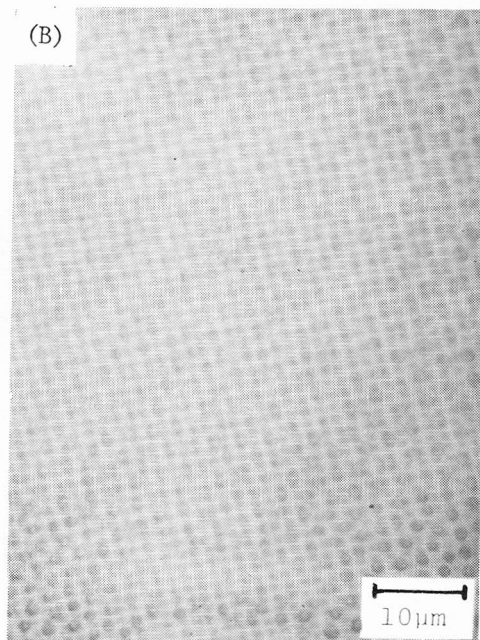
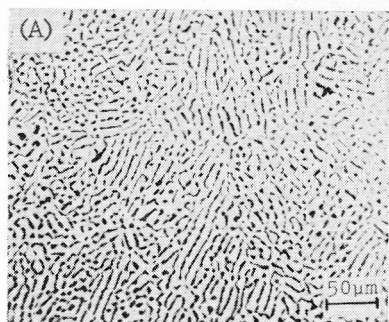


Figure 5. Microstructure of ingots solidified at 1 cm/hr. A. MgO-MgAl<sub>2</sub>O<sub>4</sub> eutectic, transverse section. B. ZrO<sub>2</sub>-MgO eutectic transverse section. C. ZrO<sub>2</sub>-SrZrO<sub>3</sub> eutectic, longitudinal section. Ref. 13 and 15.

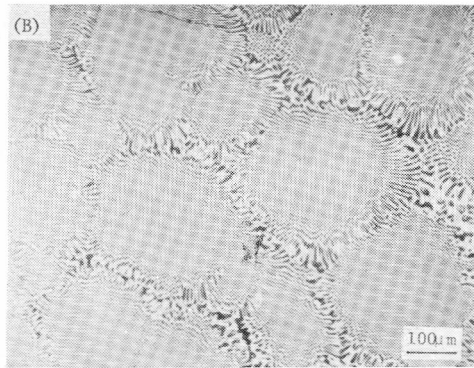
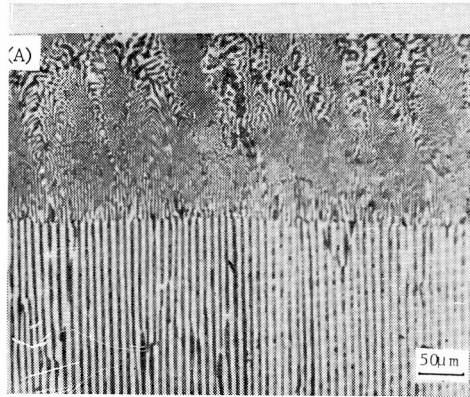


Figure 6. A. Lamellar  $ZrO_2$ - $SrZrO_3$  eutectic, quenched to show isothermal solid-liquid interface  
B.  $ZrO_2$ - $SrZrO_3$  eutectic solidified at 6 cm/hr. Colony microstructure. Ref. 15.

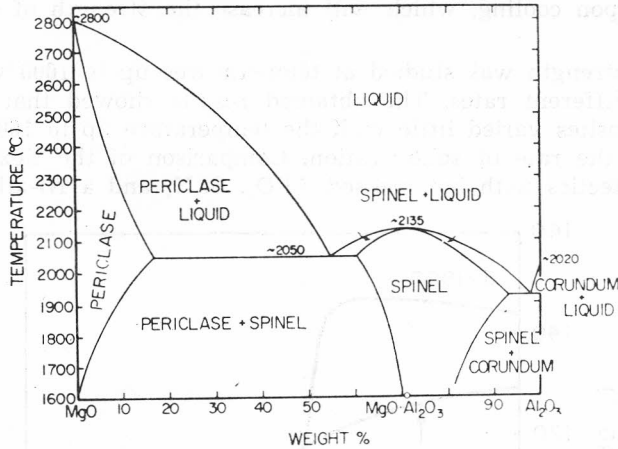


Figure 4. The system MgO-MgAl<sub>2</sub>O<sub>4</sub>. Ref. 18.

directional solidification the eutectic might be expected to yield a composite consisting of MgAl<sub>2</sub>O<sub>4</sub> (spinel) matrix reinforced with MgO whiskers. Figure 5A shows transverse section of an ingot solidified at 0.9 cm/hr where no colony microstructure is present. Similarly, colony free microstructures shown on Figure 5B and C could be obtained if ZrO<sub>2</sub>-SrZrO<sub>3</sub> and ZrO<sub>2</sub>-MgO eutectic melts were directionally solidified using relatively pure oxides and rates of solidification less than 2 cm/hr. In these cases a planar front growth was achieved as shown in the Figure 6A. Higher solidification rates always produced colony type microstructures (Figure 6B). In systems which show strong tendency towards metastability, either glass or metastable phase formation, the solidification process may not follow the equilibrium phase diagram. The metastable behavior prevents the formation of the normal eutectic microstructures as *e. g.* in the system Al<sub>2</sub>O<sub>3</sub>-SiO<sub>2</sub> and MgAl<sub>2</sub>O<sub>4</sub>-Al<sub>2</sub>O<sub>3</sub><sup>10</sup>.

With high temperature oxide eutectics the spacing ( $\lambda$ ) between rods or lamellae and the solidification rate ( $R$ ) are related by the well-known formula  $\lambda \propto R^{-1/2}$ .

The crystallographic relationships of a number of the oxide-oxide eutectics have been investigated using Laue and Buerger precession x-ray techniques. Generally we find that if both phases are cubic, the growth direction of both phases is the [111] direction with all (hkl) planes parallel. The lattice mismatch is accommodated with a dislocation network at the interface. Determination of the crystallographic relationship in more complex systems is in progress<sup>15</sup>.

### Mechanical Properties

There are several factors which could improve mechanical properties of ceramic materials with eutectic microstructures over that obtained by conventional sintering or hot pressing. Some of these factors are: (i) high strength at the high temperature of the minor phase in the whisker form (ii) stability of microstructure at high temperature (iii) the matrix phase may be placed in

compression upon cooling, which will increase the strength of eutectic composite.

Fracture strength was studied at temperatures up to 1600 °C with ingots solidified at different rates. The obtained results showed that the strength of these composites varied little with the temperature up to 1600 °C and was insensitive to the rate of solidification. Comparison of the flexural strength of ceramic eutectics with hot pressed  $\text{Al}_2\text{O}_3$ ,  $\text{Si}_3\text{N}_4$  and a Ni-alloy (Figure 7)

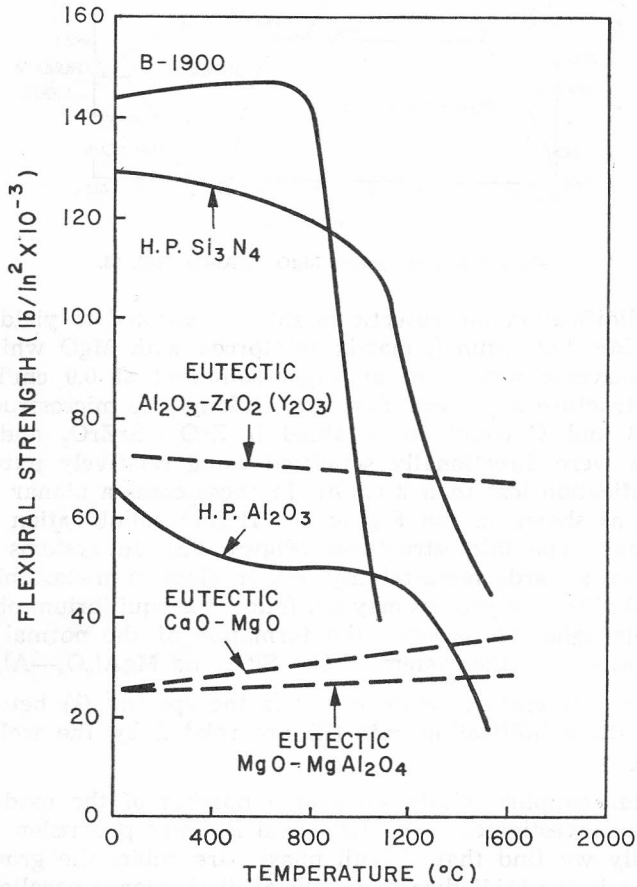


Figure 7. Flexural strength of several eutectics compared with hot pressed  $\text{Al}_2\text{O}_3$ (HP),  $\text{Si}_3\text{N}_4$ (HP) and Ni-alloy B — 1900. Ref. 11.

shows that ceramic eutectics may be some of the strongest known materials at high temperature<sup>11</sup>. A particularly interesting area for further research is determination of the fracture strength of high refractory eutectics at temperature 1600—2000 °C.

Fracture surface energies measured at room temperature for  $\text{MgO-MgAl}_2\text{O}_4$  eutectic and  $\text{ZrO}_2\text{-CaZrO}_3$  eutectic averaged to  $22 \times 10^3$  erg/cm and  $5 \times 10^4$  erg/cm respectively. At 1600 °C fracture surface energies increased to  $45 \times 10^3$  erg/cm<sup>2</sup> and  $100 \times 10^4$  erg/cm respectively. The sudden increase



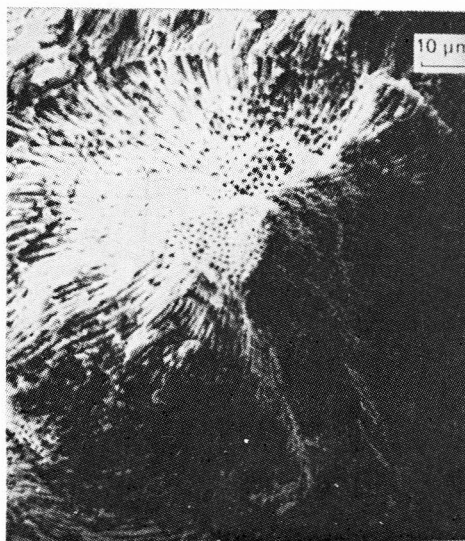


Figure 8. Fracture surface of ZrO<sub>2</sub>-MgO eutectic at room temperature. (etched with HCl). SEM photomicrograph. Ref. 15.

between 1000—1600 °C may be explained by the absorption of energy in deforming more plastic matrix and in the shear process in pulling fibers out of the matrix.

Topography of fractured surfaces was investigated with ingots fractured at different temperatures by using SEM. The effect of the fractured surface was found to be orientation dependent. In several cases the noticeable interaction between the fracture path and the microstructure was observed. Figure 8 shows deviation of crack by MgO in ZrO<sub>2</sub>—MgO eutectic ingot which was fractured at room temperature. With specimens broken at high temperatures 1200—1500 °C, which contained ductile matrix *e.g.* CaZrO<sub>3</sub>, the minor phase ZrO<sub>2</sub> was partially extracted from the ductile matrix<sup>11</sup>.

Wear resistance was measured<sup>17</sup> with SiC—B<sub>4</sub>C solidified ingots of eutectic composition. The minimum wear was found with eutectic composition at a solidification rate of approximately 9 cm/hr. The wear of the ingot of eutectic composition solidified at 9 cm/hr was considerably less than the wear of solidified B<sub>4</sub>C or hot pressed SiC (Figure 9).

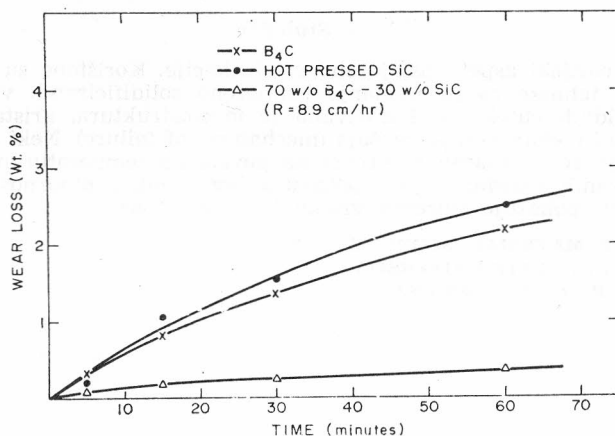


Figure 9. Wear loss of B<sub>4</sub>C-SiC eutectic compared with that of B<sub>4</sub>C and SiC. Ref. 17.

*Acknowledgments:* This work was supported by the United States Army Research Office, Durham, North Carolina, under Grant No. 8115-MC.

#### REFERENCES

1. G. Tammann, *Textbook of Metallography*, Chemical Catalog Co., New York, 1925, p. 182.
2. W. Straumanis and N. Braaks, *Z. Physik. Chem.*, **29** (1935) 30.
3. B. Chalmers, *Principles of Solidification*, John Wiley and Sons, Inc., New York, 1964, p. 194.
4. F. R. Mollard and M. C. Flemings, *Trans. Met. Soc. AIME*, **239** (1967) 526.
5. W. A. Tiller, *Liquid Metals and Solidification*, American Society for Metals, Cleveland, 1958, p. 276.
6. L. M. Hogan, R. W. Kraft and I. D. Lemkey, in *Advances in Materials Research*, Vol. 5, edited by H. Herman, Wiley — Interscience, New York, 1971, p. 83.
7. R. W. Kraft, *Trans. Met. Soc. AIME*, **221** (1961) 704.
8. J. D. Hunt and K. A. Jackson, *Trans. Met. Soc. AIME* **236** (1966).
9. D. Viehnicki and F. Schmid, *J. Mater. Sci.* **4** (1969) 84.

10. F. L. Kennard, R. C. Bradt, and V. S. Stubican, in *Reactivity of Solids, Proceedings of the 7th International Symposium on the Reactivity of Solids*, Bristol. Edited by J. S. Anderson, H. W. Roberts and F. S. Stone. Chapman and Hill, London 1972, p. 580.
11. C. Hulse and J. Batt, *Final Report to ONR Project No. 032-516/9-28-72*, May 1974.
12. D. Viechnicki, F. Schmid and J. W. McCauley, *J. Amer. Ceram. Soc.* **57** (1974) 47.
13. F. L. Kennard, R. C. Bradt, and V. S. Stubican, *J. Amer. Ceram. Soc.* **57** (1974) 566.
14. F. L. Kennard, R. C. Bradt, and V. S. Stubican, *J. Amer. Ceram. Soc.* **57** (1974) 428.
15. W. Minford, R. C. Bradt and V. S. Stubican, unpublished results.
16. F. Schmid and D. Viechnicki, *J. Mater. Sci.* **5** (1970) 470.
17. Ten-Der Hong, *M. Sc. Thesis*, The Pennsylvania State University, University Park, PA (1974).
18. A. M. Alper, R. N. McNally, P. H. Ribbe, and R. C. Doman, *J. Amer. Ceram. Soc.* **45** (1962) 263.

### SAŽETAK

#### Kristalizacija eutektičkih mikrostruktura iz oksidnih i karbidnih talina

V. S. Stubičan

Opisan je teorijski aspekt usmjerene solidifikacije. Korištene su dvije različite eksperimentalne tehnike za pripremanje usmjereno solidificiranih visoko otpornih oksidnih i karbidnih eutektika. Istraživana je mikrostruktura, kristalografija, mehanička svojstva i mehanizam promašaja (mechanism of failure). Neki od istraživanih eutektikuma zadržavaju znatnu otpornost na povišenim temperaturama, dok većina slitina i sintrovanih oksidnih tijela pokazuju brz gubitak otpornosti. Eutektik u sistemu  $B_4C-SiC$  pokazuje izuzetno visoku i trajnu otpornost.

DEPARTMENT OF MATERIAL SCIENCES  
THE PENNSYLVANIA STATE UNIVERSITY  
UNIVERSITY PARK, PA 16802 USA